Impacts of APEC-based Nodal Analysis on Pin Power Reconstruction

Sungju Kwon[a], Joo Il Yoon[b] and Yonghee Kim[a]
[a]*Department of Nuclear & Quantum Engineering, KAIST, Daejeon, Republic of Korea*
[b]*KEPCO NF, 242, 989 beon-gil, Daedeokdae-ro, Yuseong-gu, Daejeon, Republic of Korea*
Corresponding author: sjukwon@knfc.co.kr

1. Introduction

The coarse mesh nodal method, which has been widely used in core analysis recently, provide average power of fuel assembly (FA) as a result of core analysis while required nuclear design data for safety analysis is pin power distribution of the FA. As shown in Figure 5, pin power distribution can be estimated by multiplying the normalized homogeneous power distribution and heterogeneous form function. Homogeneous power distribution is calculated using the homogeneous flux distribution in the node. Homogeneous flux distribution can be produced using the nodal calculation results, and the form function can be obtained from the lattice calculation results. Therefore, if the accuracy of the nodal calculation result is improved, reconstructed pin power using the results is also more accurate.

Recently, APEC method has been developed for more accurate core analysis. In the APEC method, an FA two-group XS is expressed as a simple polynomial function of the assembly-wise current-to-flux ratio (CFR) and the fast-to-thermal flux ratio called the spectral index (SI). As a result, it was confirmed that nodal calculation accuracy is improved [1].

In this paper, form function method is used to confirm the impacts of APEC based nodal results on pin power reconstruction (PPR). The homogeneous flux is calculated using the APEC based nodal calculation results and basis function used in AFEN method [2], and form function is obtained from the single FA lattice calculation results. Finally, PPR is performed using AEPC based nodal calculation results to SMR initial core and the results is analyzed.

2. Determination of homogeneous flux distribution

2.1 Analytic solution of two dimensional diffusion equation

In the two-dimensional node, homogeneous flux distribution can be directly obtained using the solution of two energy group diffusion equation.

$$-D_1\nabla^2\phi_1(x,y)+\Sigma_{R1}\phi_1(x,y)=\frac{1}{k}\nu\Sigma_{f1}\phi_1(x,y)+\left(\frac{1}{k}\nu\Sigma_{f2}+\Sigma_{12}\right)\phi_2(x,y) \quad (1)$$

$$-D_2\nabla^2\phi_2(x,y)+\Sigma_{R2}\phi_2(x,y)=\Sigma_{21}\phi_1(x,y) \quad (2)$$

In the equation (1) and (2), homogenized cross sections and effective multiplication factor can be obtained from the nodal calculation results. Since the equations for each energy group are coupled to the different energy group, it is impossible to get directly analytic solution of two group diffusion equation. Thus, similarity transformation matrix R is defined as follows:

$$R_n=\begin{bmatrix} r_1 & r_2 \\ 1 & 1 \end{bmatrix} \quad \text{where, } r_i=\left(\frac{\Sigma_{R2}-\lambda_i D_2}{\Sigma_{21}}\right)$$

Using the matrix R_n, the eigenvalues of equations (1) and (2) can be calculated as follows:

$$\lambda_1=\frac{1}{2}(\alpha-\beta), \quad \lambda_2=\frac{1}{2}(\alpha+\beta)$$

Where,

$$\alpha=\frac{\left\{D_2\left(\Sigma_{R1}-\frac{1}{k}\nu\Sigma_{f1}\right)+D_1\Sigma_{a2}\right\}}{D_1D_2}$$

$$\beta=\frac{\sqrt{\left\{D_2\left(\Sigma_{R1}-\frac{\nu}{k}\Sigma_{f1}\right)-D_1\Sigma_{a2}\right\}^2+4D_1D_2\left(\Sigma_{12}\Sigma_{21}+\frac{\nu}{k}\Sigma_{f2}\Sigma_{21}\right)}}{D_1D_2}$$

The new unknown ξ is defined as follows using the matrix R_n.

$$\vec{\xi}(x,y)=(R_n)^{-1}\vec{\phi}(x,y) \quad (3)$$

Where,

$$\vec{\phi}(x,y)=\begin{bmatrix}\phi_1(x,y)\\ \phi_2(x,y)\end{bmatrix}, \quad \vec{\xi}(x,y)=\begin{bmatrix}\xi_1(x,y)\\ \xi_2(x,y)\end{bmatrix}$$

Finally, equation (1) and (2) can be written as Helmholtz equations where the two energy groups are decoupled.

$$\nabla^2\xi_g(x,y)=\lambda_g\xi_g(x,y), \quad g=1,2 \quad (4)$$

The general solution of equation (4) is well known follows [2]:

$$\xi_g(x,y)=C_1sn(\kappa_g x)+C_2cn(\kappa_g x)+C_3sn(\kappa_g y)+C_4cn(\kappa_g y)+$$
$$C_5sn\left(\frac{\kappa_g}{\sqrt{2}}x\right)cn\left(\frac{\kappa_g}{\sqrt{2}}y\right)+C_6sn\left(\frac{\kappa_g}{\sqrt{2}}x\right)sn\left(\frac{\kappa_g}{\sqrt{2}}y\right)+$$

$$C_7 cn\left(\frac{\kappa_g}{\sqrt{2}}x\right)sn\left(\frac{\kappa_g}{\sqrt{2}}y\right)+C_8 cn\left(\frac{\kappa_g}{\sqrt{2}}x\right)cn\left(\frac{\kappa_g}{\sqrt{2}}y\right) \quad (5)$$

With $\kappa_i=\sqrt{|\lambda_i|}$ while *sn* and *cn* represent functions determined in accordance with the sign of λ_i

$$sn(\kappa_i u)=\begin{cases}\sin(\kappa_i u)\\ \sinh(\kappa_i u)\end{cases},\ cn(\kappa_i u)=\begin{cases}\cos(\kappa_i u) & \lambda_i>0\\ \cosh(\kappa_i u) & \lambda_i<0\end{cases}$$

Coefficients of Equation (5) can be determined using eight boundary conditions then, the analytical solution of equation (1) and (2) can be get by equation (3). Generally, the average fluxes in the four surfaces and corners of the node are used as boundary conditions. The average fluxes in the four surfaces can be directly obtained from nodal calculation results. However, the corner fluxes of the node are not generated in nodal calculation.

2.2 Calculation of corner point flux of the node

To calculate the corner point flux, above all, it is necessary to set the four corners and surfaces of a node. Figure 1 shows notation of the corners and surfaces of the node.

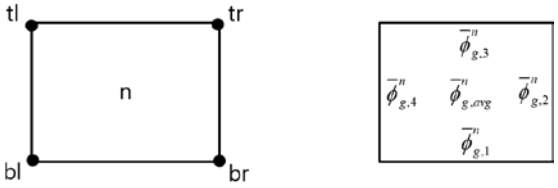

Figure. 1. Notation of the corner and surface of the node

The MSS (Method of Successive Smoothing) is used to calculate the corner point flux. The corner point fluxes in the node are approximated by assuming that flux distribution in the node are separable [3]:

$$\phi^n_{g,bl}(x,y)=\frac{\bar{\phi}^n_{g,1}(x)\times\bar{\phi}^n_{g,4}(y)}{\bar{\phi}^n_g} \quad (6)$$

Where one-dimensional fluxes and node average flux can be obtained from nodal solution. Then, the average flux in the common corner to four nodes is determined by the average of the four estimative of the heterogeneous flux in the corners:

$$\bar{\phi}^n_{g,bl}(x,y)=\frac{1}{4}\left(\begin{array}{l} f^n_{g,bl}\dfrac{\bar{\phi}^n_{g,1}(x)\times\bar{\phi}^n_{g,4}(y)}{\bar{\phi}^n_g}+f^{n+1}_{g,br}\dfrac{\bar{\phi}^{n+1}_{g,1}(x)\times\bar{\phi}^{n+1}_{g,2}(y)}{\bar{\phi}^{n+1}_g}\\ +f^{n+2}_{g,tr}\dfrac{\bar{\phi}^{n+2}_{g,2}(x)\times\bar{\phi}^{n+2}_{g,3}(y)}{\bar{\phi}^{n+2}_g}+f^{n+3}_{g,tl}\dfrac{\bar{\phi}^{n+3}_{g,3}(x)\times\bar{\phi}^{n+3}_{g,4}(y)}{\bar{\phi}^{n+3}_g}\end{array}\right) \quad (7)$$

Where $f^{n+i}_{g,jk}$ (i= 0 to 3, g = t or b, k = l or r) are discontinuity factors on the corner of the nodes and it can be obtained from lattice calculation. In this paper, discontinuity factor is set to unity. Thus, corner point flux of equation (7) is not heterogeneous flux. Optimized discontinuity factor will be used in further study.

2.3 Addition constant term to the analytic solution

If the analytic solution as equation (5) is not used to solve the diffusion equation in the nodal calculation, the homogeneous flux distribution produced using analytic solution does not preserve the node reaction rate of the nodal calculation results even if nodal calculation results are used as boundary condition. Because the flux distributions produced in the node by different solution of diffusion equation cannot exactly match each other. This problem can be solved by using the node average flux as an additional boundary condition. Thus, equation (8) is obtained by adding constant term to equation (5).

$$\begin{aligned}\xi_g(x,y)=&C_1 sn(\kappa_g x)+C_2 cn(\kappa_g x)+C_3 sn(\kappa_g y)+C_4 cn(\kappa_g y)+\\ &C_5 sn\left(\frac{\kappa_g}{\sqrt{2}}x\right)cn\left(\frac{\kappa_g}{\sqrt{2}}y\right)+C_6 sn\left(\frac{\kappa_g}{\sqrt{2}}x\right)sn\left(\frac{\kappa_g}{\sqrt{2}}y\right)+\\ &C_7 cn\left(\frac{\kappa_g}{\sqrt{2}}x\right)sn\left(\frac{\kappa_g}{\sqrt{2}}y\right)+C_8 cn\left(\frac{\kappa_g}{\sqrt{2}}x\right)cn\left(\frac{\kappa_g}{\sqrt{2}}y\right)+C_9\end{aligned} \quad (8)$$

2.4 Determination of coefficients

There are nine coefficients in equation (8) and those can be determined by nine boundary conditions. Four surface average fluxes and a node average flux can be obtained directly from the nodal calculation results, and four corner point fluxes can be calculated using method of section 2.2.

3. Pin Power Reconstruction for SMR initial core

3.1 SMR initial core

Figure 2 shows that six types of 17 × 17 FAs (Fuel Assemblies) are loaded in the SMR (Small Modular Reactor) core. For the A2- and A3-type FAs, U enrichment is 2.8 wt% and it is about 4.9 wt% for other FAs. In the previous study [1], three different core calculations have been performed for the SMR core. The first is the nodal calculation using the FWC-ADF method, the second is the nodal calculation using APEC method, and the last is the reference core calculation using DeCART2D [4].

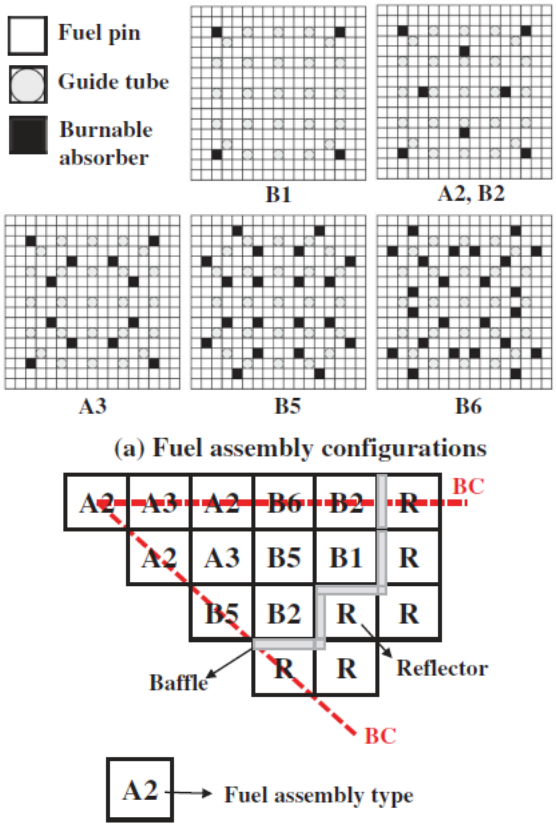

Figure 2. SMR initial core and loaded fuel assembly configurations

Group	FA type	A2			
	XS type	D	Σ_R	$\nu\Sigma_f$	$\Sigma_{s\to s'}$
Fast	(1)	1.5615	0.0244	0.0061	0.0017
	(2)	-0.15%	0.65%	0.21%	-0.28%
	(3)	0.04%	0.03%	0.06%	-0.01%
Thermal	(1)	0.4017	0.0815	0.1188	0.0155
	(2)	-0.02%	0.03%	0.07%	0.78%
	(3)	0.00%	0.01%	0.01%	0.04%

Group	FA type	B1			
	XS type	D	Σ_R	$\nu\Sigma_f$	$\Sigma_{s\to s'}$
Fast	(1)	1.5562	0.0246	0.0087	0.0022
	(2)	0.68%	1.15%	-0.02%	-0.03%
	(3)	0.07%	-0.09%	-0.02%	-0.03%
Thermal	(1)	0.4008	0.1081	0.1850	0.0144
	(2)	-0.38%	0.82%	0.87%	-0.11%
	(3)	0.00%	0.03%	0.02%	-0.11%

(1) Reference
(2) (ADF-FWC - Ref.)/Ref. (%)
(3) (APEC - Ref.)/Ref. (%)

Figure 3. Difference of equivalence constants from reference and each nodal method

Figure 3 shows the difference of equivalence constants from reference and each nodal method. A2 FA is located center and B1 FA is located near the reflector, respectively. In FWC-ADF based nodal method, equivalence constants obtained from single FA lattice calculation are used for nodal calculation. When the APEC nodal method is applied, equivalence constants are updated during nodal calculation using actual leakage information. Thus, equivalence constants get closer to reference values using APEC function.

Figure 4 shows the relative power density (RPD) of FAs from reference and each nodal calculation. The RPD of FA obtained by FWC-ADF and APEC based nodal calculation shows maximum error of -2.45% and 0.73%, respectively, compared with the reference RPD. The RPD error does not exceed 1% when APEC method is applied.

(1)
(2)
(3)

1.3464	1.2352	1.1827	1.0576	0.8773
-2.16	-2.45	-0.90	-0.25	2.38
-0.67	-0.65	-0.41	0.33	0.15
	1.2638	1.0509	1.0149	0.761
	-1.62	-0.60	0.30	2.18
	-0.65	-0.05	0.00	0.71
		1.0616	0.7908	
		-0.50	1.85	
		-0.29	0.73	

(1) Reference
(2) (ADF-FWC - Ref.)/Ref. (%)
(3) (APEC - Ref.)/Ref. (%)

Keff	
Reference	1.14424
ADF-FWC	1.14603
APEC	1.14424

Figure 4. Relative power density and effective multiplication factor of reference and each nodal calculation results (octant core)

3.2 PPR calculation procedure

By determining the coefficients of equation (8) using APEC based nodal calculation results, the homogeneous flux distribution in the node can be obtained. Then, since nodal calculation is performed for FA which is divided into 2x2 nodes, the homogeneous flux distribution of the FA is reconstructed using the homogeneous flux distribution of each node. Homogeneous pin power distribution can be calculated using determined homogeneous flux distribution and $\kappa\Sigma_f$, and the results are normalized and multiplied by form function. Finally, the RPD obtained from nodal calculation is multiplied by each pin to finalize the PPR calculation. Figure 5 shows PPR calculation procedure.

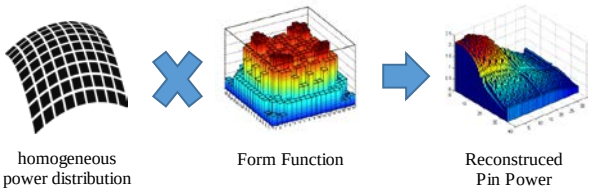

Figure 5. Pin power reconstruction calculation procedure

3.3 Results and Analysis

The PPR is performed using FWC-ADF and APEC based nodal calculation results, respectively according to the section 3.2. PPR was performed only for FAs

with relatively large differences between (2) and (3) in Figure 5. In this way, the impacts of PPR using the APEC based nodal calculation results as boundary condition can be more clearly analyzed. Figure 6 shows the maximum, minimum and RMS error between reconstructed pin power and reference pin power.

Max	**0.00%**	**0.00%**	**-**	**-**	**11.12%**
Min	**-3.25%**	**-7.87%**	**-**	**-**	**-2.38%**
RMS	**2.11%**	**2.78%**	**-**	**-**	**2.65%**
Position	**(1,1)**	**(3,3)**	**-**	**-**	**(9,17)**
		-	**-**	**-**	**12.51%**
		-	**-**	**-**	**-3.95%**
		-	**-**	**-**	**2.79%**
		-	**-**	**-**	**(17,17)**
			-	**13.21%**	
			-	**-3.01%**	
			-	**2.51%**	
			-	**(17,17)**	

(a) FWC-ADF based PPR

Max	**0.00%**	**0.45%**	**-**	**-**	**8.38%**
Min	**-1.68%**	**-6.01%**	**-**	**-**	**-4.51%**
RMS	**0.71%**	**1.38%**	**-**	**-**	**1.70%**
Position	**(1,1)**	**(3,3)**	**-**	**-**	**(9,17)**
		-	**-**	**-**	**10.74%**
		-	**-**	**-**	**-6.09%**
		-	**-**	**-**	**2.35%**
		-	**-**	**-**	**(17,17)**
			-	**11.13%**	
			-	**-5.15%**	
			-	**2.15%**	
			-	**(17,17)**	

(b) APEC based PPR

Figure 6. Reconstructed pin power error between PPRs and reference

The maximum (or minimum) error of the pin power occurred near the node edge except the A3 FA adjacent center fuel. In case of A3 FA, it occurred at the position of burnable absorber, not around the corner. Especially, since discontinuity factor is set to 1 in the calculation of corner point flux, there is a large error in vicinity of the vertex of FA. If discontinuity factor is optimized, the error near the vertex will be reduced.

If the homogeneous flux distribution and form function are exactly equal to the reference solution in the PPR calculation, the RMS errors in Figure 6 should be almost zero. Therefore, the PPR error is caused by the error of the nodal calculation results used as boundary condition and the inaccuracy of the form function obtained by the single FA lattice calculation. Of course, there is an error in calculating the homogeneous flux distribution, but it is relatively small.

The RMS error of the FAs located core inner region is reduced similar to the improved PRD error using the APEC method. However, although the RPD error of FA was greatly improved in vicinity of the reflector, the RMS error of the FA did not decrease as expected. It means that even if the homogeneous flux distribution is improved using the APEC based nodal calculation results, there is no significant change of the PPR error due to inaccuracy of the form function produced by the single FA lattice calculation. However, fortunately, APEC function is produced by several color-set calculation, so more accurate form function can be used to PPR. The form function from color-set calculation will be used in further study.

4. Conclusions

Pin power reconstruction can be performed using homogeneous flux distribution in the node and form function. The homogeneous flux distribution in the node was obtained using an analytic solution of the two group diffusion equation. Then, in order to preserve the reaction rate of the node, constant term is added to the analytic solution. The pin power reconstruction was performed through APEC based nodal calculation for the SMR initial core. As a result, the improvement effect of RMS error for FAs in inner core region was significant, whereas, the improvement effect of RMS error for FAs in outer core region was not significant due to inaccuracy of form function. To solve this problem, we can use the improved form function which can be obtained from the result of the color-set calculation used to produce the APEC function.

REFERENCES

[1] W. Kim, K. Lee & Y. Kim, “Functionalization of the Discontinuity Factor in the Albedo-Corrected Parameterized Equivalence Constants (APEC) Method,” ANS, July 2018.
[2] J. M. Noh and N. Z. Cho, “A New Approach of Analytic Basis Function Expansion to Neutron Diffusion Nodal Calculation,” November, 1993.
[3] Smith. K. S., and Henry. A. F., “SIMULATE-3 Pin Power Reconstruction: Methodology and Benchmarking,”, *Proc. Int. Reac. Phys. Conf.*, Jackson Hole, Wyoming, Sep. 1988, Vol. III. pp. 18. (1988)
[4] J. Y. Cho, DeCART2Dv1.1 User’s Manual, KAERI/UM-40/2016, 2016.